



Effect of the interfacial tension and ionic strength on the thermodynamic barrier associated to the benzocaine insertion into a cell membrane



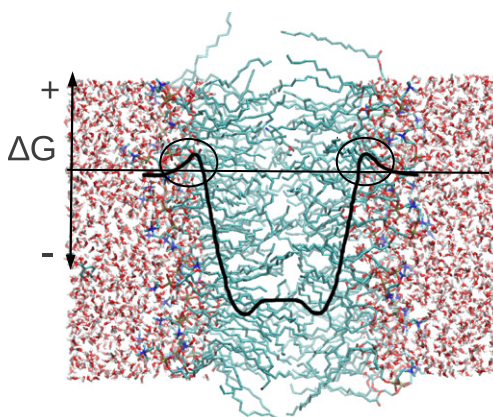
J.J. López Cascales*, S.D. Oliveira Costa

Universidad Politécnica de Cartagena, Grupo de Bioinformática y Macromoléculas (BioMac) Aulario II, Campus de Alfonso XIII, 30203 Cartagena, Murcia, Spain

HIGHLIGHTS

- The insertion of benzocaine into a phospholipid bilayer is a spontaneous process.
- A thermodynamic barrier was evidenced at the bilayer/water interface.
- This barrier diminishes with the fraction of charged lipid in the bilayer.
- The ionic strength diminishes as well this thermodynamic barrier.
- The interfacial tension plays a crucial role in this thermodynamic barrier.

GRAPHICAL ABSTRACT



ARTICLE INFO

Article history:

Received 16 November 2012
Received in revised form 4 December 2012
Accepted 5 December 2012
Available online 20 December 2012

Keywords:

Local anaesthetics
Benzocaine
Free energy
Bilayers
Interfacial tension
MD simulations

ABSTRACT

The insertion of local anaesthetics into a cell membrane is a key aspect for explaining their activity at a molecular level. It has been described how the potency and response time of local anaesthetics is improved (for clinical applications) when they are dissolved in a solution of sodium bicarbonate. With the aim of gaining insight into the physico-chemical principles that govern the action mechanism of these drugs at a molecular level, simulations of benzocaine in binary lipid bilayers formed by DPPC/DPPS were carried out for different ionic strengths of the aqueous solution. From these molecular dynamic simulations, we observed how the thermodynamic barrier associated with benzocaine insertion into the lipid bilayers diminished exponentially as the fraction of DPPS in the bilayer increased, especially when the ionic strength of the aqueous solution increased. In line with these results, we also observed how this thermodynamic barrier diminished exponentially with the phospholipid/water interfacial tension.

© 2012 Elsevier B.V. All rights reserved.

1. Introduction

The clinical potency of local anaesthetics (LA) often depends on two facts: their vascular absorption and their distribution in the

tissue surrounding the site of deposition. The ability to partition the anaesthetic molecules into various compartments is a crucial aspect related with their activity from a molecular point of view. In this context, local anaesthetics, like many neuroactive drugs, must penetrate into, or pass through the neuronal plasma membrane to be pharmacologically active [1,2]. Furthermore, in clinical local anaesthetic procedures, the pharmacological drugs must pass through the perineum, which is composed of fibrous and cellular barriers before reaching the

* Corresponding author. Tel.: +34 968325567; fax: +34 968325931.
E-mail address: javier.lopez@upct.es (J.J. López Cascales).

nerve fibres. Hence, membrane permeation and adsorption processes control LA penetration and their resulting concentration at the intended site of action [2].

Certain liposoluble LA in physiological conditions may present a non-protonated (neutral) and protonated (charged) form, where the non-protonated form have been observed to be more membrane-permeant than the protonated one, enhancing it to pass through the hydrophobic barrier of the membrane [3,4]. In this regard, the clinical use of local anaesthetic dissolved in a sodium bicarbonate buffer has been widely used because, it attenuates the pain involved in skin infiltration [5], and together, they produce a more rapid onset and a decrease in the minimum concentration required to achieve a therapeutic dose [6], bearing in mind the high pKa of most such pharmacological species, which range from 7.7 for the mevipacaine to 9.8 for the piperocaine [2,6]. Thus, for example, the clinical effects of bupivacaine and lidocaine are strengthened (and hence, their dosage reduced) when they are administered dissolved in a sodium bicarbonate buffer [5]. However, the contribution of the ionic strength of the sodium bicarbonate solution (sodium concentration) to the activity of these anaesthetics has, to date, been ignored. In this context, this work focuses on the effect of the ionic strength (sodium concentration) of an aqueous solution on the insertion process of benzocaine into a lipid bilayer composed of different fractions of charged lipids. In this regard, the cell membrane was modelled by symmetric binary lipid bilayers formed of dipalmitoylphosphatidylcholine (DPPC) and dipalmitoylphosphatidylserine (DPPS), where the DPPC is a neutral phospholipid, the DPPS is a phospholipid which bears a negative charge in physiological conditions, and benzocaine is a non-charged liposoluble local anaesthetic in physiological conditions due to its low pKa of 3.5 (in this regard, the effect associated with the hydrolysis of the anaesthetic can be discarded) [4,7,8], and where it was ignored the presence of other important molecules in our model of cell membrane, such as the presence of cholesterol. Molecular dynamics simulation was used to carry out the present study.

In previous investigations carried out by our group [9,10], it was determined how the insertion of benzocaine into lipid bilayers is a spontaneous process from a thermodynamic point of view, in which entropy is the driving thermodynamic force responsible of this spontaneous process [10]. Furthermore, the existence of a thermodynamic barrier during the benzocaine insertion into the cell membrane was determined. This barrier, located at the lipid/water interface, diminished as the fraction of charged lipids in the lipid bilayer increased [10]. Keeping in mind the results mentioned above, this work looks at how the ionic strength of the aqueous solution affects the insertion of benzocaine into a lipid bilayer, concentrating on two main aspects:

- 1 The effect of the ionic strength on the thermodynamic barrier associated with benzocaine insertion into a lipid bilayer.
- 2 How the interfacial tension between the phospholipid bilayer and the aqueous solution plays a crucial role in diminishing this thermodynamic barrier.

2. Model and methods

2.1. Model

Five different lipid bilayers were generated with the goal of analysing the full range of lipid compositions of a binary bilayer composed of DPPC and DPPS. The starting system was formed by a bilayer composed of 72 DPPC molecules (36 DPPC per leaflet) and 5042 water molecules of the SPC water model [11]. A precise description of how the three dimension periodical box was generated is given elsewhere [12–14,9]. Once this bilayer of DPPC was generated, four additional bilayers were constructed by substituting 12, 24, 48 and 72 DPPC molecules with 12, 24, 48 and 72 DPPS molecules. To balance the negative charge associated to each DPPS molecule under physiological conditions, 12, 24, 48 and 72 sodium ions (Na^+) were

introduced into the system by substituting water molecules with sodium ions. In summary, five different binary bilayer of DPPC:DPPS were generated with the following compositions 72:0, 60:12, 48:24, 24:48 and 0:72.

The molecular fraction of DPPS that forms the lipid bilayer, χ , was defined as follows:

$$\chi = \frac{n_{\text{DPPS}}}{n_{\text{DPPC}} + n_{\text{DPPS}}} \quad (1)$$

where χ represents the molecular fraction of DPPS (n_{DPPS}) with respect to the total number of lipids in the bilayer ($n_{\text{DPPC}} + n_{\text{DPPS}}$).

Finally, to simulate a 0.5 N NaCl concentration in the aqueous solution, a water molecule was randomly substituted by one sodium and one chloride ion, respectively, every 111 water molecules in each of the systems generated above (after considering the following approximation: 0.5 N (NaCl) = 0.5 M (NaCl) = 0.5 moles (NaCl)/1 (litre of solution) \approx 0.5 moles (NaCl)/1 kg (H_2O) = 0.5 moles (NaCl)/55.6 moles H_2O , i.e., we obtain a ratio of 1(Na^+):111(H_2O), and the same for the Cl^-).

2.2. Simulation parameters

The GROMACS 3.3.3 package [16,17] was used to perform the molecular dynamic simulations, with a constant integration time step of 2 fs. The electrostatic contribution was calculated using a long range electrostatic interaction by the Particle Mesh Ewald method [18,19], in which all the coordinates of the simulated trajectories were recorded every 5 ps of simulation time. Bond lengths were constrained using the LINCS algorithm [20]. All the simulation boxes were coupled to an external pressure and temperature bath, using the Berendsen algorithm [21], with temperature and pressure coupling constants of 0.1 and 1 ps, respectively. Due to the anisotropy of the membranes along the Z-axis, all the simulations were carried out using a semi-isotropic pressure algorithm coupling bath. The simulated trajectory lengths were of 100 ns, where the first 10 ns of each simulation were discarded for analysis because this was the time required by the systems to achieve an equilibrated state. All the simulations were carried out at 350 K, a temperature that was chosen because it is above the transition temperature of 314 K [22] and 326 K [23] for pure bilayers of DPPC and DPPS, and also because this temperature is above the transition temperature of all the binary bilayers formed by DPPC/DPPS, as deduced from the corresponding experimental phase diagram [24]. In short, the temperature of 350 K ensures that all these binary bilayers are in liquid crystalline state, regardless of the fraction of DPPS in the lipid bilayer. The molecules of DPPC and DPPS were simulated using the force field employed in previous simulations of lipid bilayers formed exclusively of DPPC [25] and DPPS [12]. As in previous articles in which DPPS was involved in our simulations [13,26,27], the charge distribution of DPPS and of the rest of species with net charge were reduced by a factor of two to compensate, in part, the absence of polarizability in our models. This reduction that has been effective in the study of soap/alcohol/water interfaces, biological membranes and micelles [25,28] is based, in short, to the fact that coulombic interactions in these systems are exaggerated due to the insufficient screening performance of the SPC [11] water model used in our simulations.

Benzocaine was modelled as in previous simulations [9,10], where Fig. 1 shows the charge distribution used to simulate this molecule. The bond distances, angles, and LJ parameters were taken from the standard GROMOS-87 force field [29].

Since calculation of the lateral pressure profile needs much computing power, the trajectories generated using the Particle Mesh Ewald method were employed to recalculate the pressure tensor of Eq. (10) using the cut-off method rather than the Particle Mesh Ewald method mentioned above. In the process of calculating the lateral pressure profile, short and long spherical cutoffs of 1.4 and

1.8 nm were used for re-calculating the non-bonded forces, according to previous simulations carried out by other authors [30–32]. Thus, while the list of atoms inside the short cutoff was updated and their interactions were calculated every time step, the list of neighbouring atoms between the short and long cutoffs was updated and their interactions calculated every ten time steps. In an attempt to avoid any mismatch between these two ways of calculating the electrostatic interactions, several simulations were carried out at different ϵ_r , and almost the same results were obtained for the surface area per lipid, using the Particle Mesh Ewald or the cut-off method, when $\epsilon_r = 1.1$. To a certain extent, this result was expected from previous simulations involving the cut-off method rather than the Particle Mesh Ewald method to calculate the electrostatic interactions because the electrostatic interaction was overestimated due to the absence of polarizability in the atomic models used in our simulations, as mentioned, too, by Berendsen et al. in several of their papers [25].

3. Results and discussion

3.1. Free energy profile, $\Delta G(z)$

The umbrella sampling method [33] was used to evaluate the free energy profile associated with benzocaine insertion into a lipid bilayer. The relationship between the free energy profile and the potential mean force is depicted in the following equation,

$$\Delta G_b(z) = -RT \ln \frac{C_b^{\text{eq}}(z)}{C_b^*} = PMF \quad (2)$$

where $\Delta G_b(z)$ represents the free energy profile along the z -axis perpendicular to the bilayer, R the constant of the gases, T the temperature, $C_b^{\text{eq}}(z)$ the concentration profile of the benzocaine along the z -axis, C_b^* the concentration of benzocaine in the solution (aqueous solution in our case) and PMF the potential of mean force computed with respect to a reaction coordinate equal to the z coordinate of the centre of mass of the benzocaine molecule, using the umbrella algorithm and WHAM method (Weight Histogram Analysis Method) [34]. Since an accurate profile of $C_b^{\text{eq}}(z)$ could not be obtained during the simulation time, a biasing potential was applied to the benzocaine. In this respect, 36 independent simulations of 50 ns each were performed, for each of the ten systems studied in this work, which amounts a total of 18,000 ns of simulation time. Each of the 36 simulations for all the systems studied, the benzocaine was restrained at a given depth in the bilayer by a harmonic potential on the z -coordinate perpendicular to the membrane plane, leaving it to move freely on the membrane plane. The force constant of this harmonic spring was $3000 \text{ kJ} \cdot \text{mol}^{-1} \text{ nm}^{-2}$ for all the restrained positions of the benzocaine across the membrane. Thus, benzocaine was shifted by 0.1 nm between consecutive simulation

windows. Following the same methodology as in previous works [9,35–37], two benzocaine molecules were introduced into the system to save computing time. The separation was 3.5 nm along the z axis to ensure the absence of correlations between both molecules. Obviously, and as a first approximation, in this study it was discarded the possibility that benzocaine can form aggregates despite the tendency of the benzocaine to form molecular aggregates depending of its concentration.

Fig. 2 depicts a schematic representation of the free energy profile associated with the insertion of benzocaine into a lipid bilayer formed only by DPPC, in the absence of salt. The figure clearly illustrates the existence of a thermodynamic barrier associated with the insertion of the benzocaine into the lipid/solution interface, and a minimum in the free energy located in the interior of the hydrocarbon zone of the lipid bilayer.

Fig. 3 shows the free energy profiles associated with the insertion of benzocaine as a function of the lipid bilayer composition, in the absence and the presence of salt in the solution. In all cases, a minimum in the free energy profile is located in the hydrocarbon region within the lipid bilayer. This minimum value for the free energy of $-24 \pm 2 \text{ kJ/mol}$ and $-28 \pm 2 \text{ kJ/mol}$ in the absence and the presence of salt, respectively, becomes more negative for $\chi = 1$ (bilayers exclusively formed of DPPS), in which values of -28.3 ± 0.2 and $-31.8 \pm 1.1 \text{ kJ/mol}$ were measured, in the absence and presence of salt, respectively. These simulation data agree with the experimental data reported by Matsuki et al. [4] for the insertion of a local anaesthetic in DPPC bilayers ($25\text{--}30 \text{ kJ/mol}$).

The free energy profiles associated to different compositions of the lipid bilayer can be in part associated to the difference in the free space in the interior of the membrane related with the deuterium order parameters of the hydrocarbon lipid tails such as it was obtained in a previous article [10], i.e., to the variation in the viscosity in the interior of the lipid bilayer, according with the comments of one of the reviewers of this work.

In this context, and focusing our interest on the free energy barrier associated with benzocaine insertion into the bilayer (such as can be observed in Fig. 2), Fig. 4 shows a semi-logarithmic plot of the barrier with the bilayer composition χ , in the absence and presence of salt in the aqueous solution. Fitting these points to a straight line gives a linear equation for these representations as follows:

$$\ln(\Delta G_{\text{max}})_{\text{without NaCl}} = -2.93\chi + 1.48, \quad (3)$$

$$\ln(\Delta G_{\text{max}})_{0.5 \text{ N NaCl}} = -2.48\chi + 0.19 \quad (4)$$

or, expressed in their exponential form,

$$(\Delta G_{\text{max}})_{\text{without NaCl}} = 4.39e^{-2.93\chi}, \quad (5)$$

$$(\Delta G_{\text{max}})_{0.5 \text{ N NaCl}} = 1.21e^{-2.48\chi}, \quad (6)$$

where ΔG is expressed in kJ/mol.

These results confirm that an increase in the DPPS content of the lipid bilayer facilitates the insertion of the benzocaine into the lipid bilayer by weakening the free energy barrier located in the lipid/solution interface. This result may be related with the experimental evidence that the activity of certain local anaesthetics is modulated by the DPPS composition of the cellular membrane (as corresponds to most of the cells of the central nervous system compared with other eukariotic cells). Thus, Baenziger et al. [38] reported how the presence of charged lipids in the membrane enhances the drug activity by increasing the partitioning of tetracaine into the lipid bilayer, which is in a good agreement with our findings. However, from a physico-chemical point of view, some aspects need to be explained in line with this anomalous behaviour: The free energy barrier related to the insertion of benzocaine (a neutral molecule) into a lipid bilayer becomes smaller as the charge density in the lipid/water interface increases. The next step was to try to provide a suitable explanation for

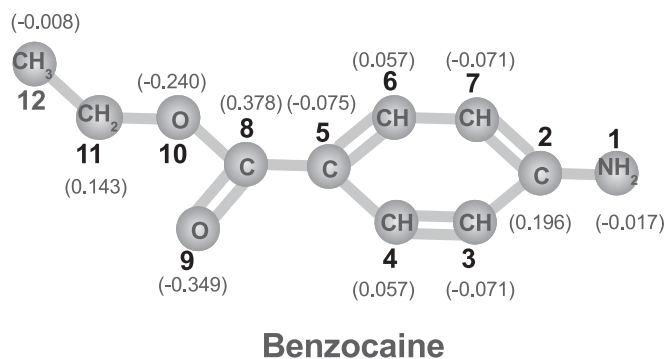


Fig. 1. Benzocaine model used in this work. The atomic charge distribution (in e units) was calculated using the semi-empiric CNDO method [15].

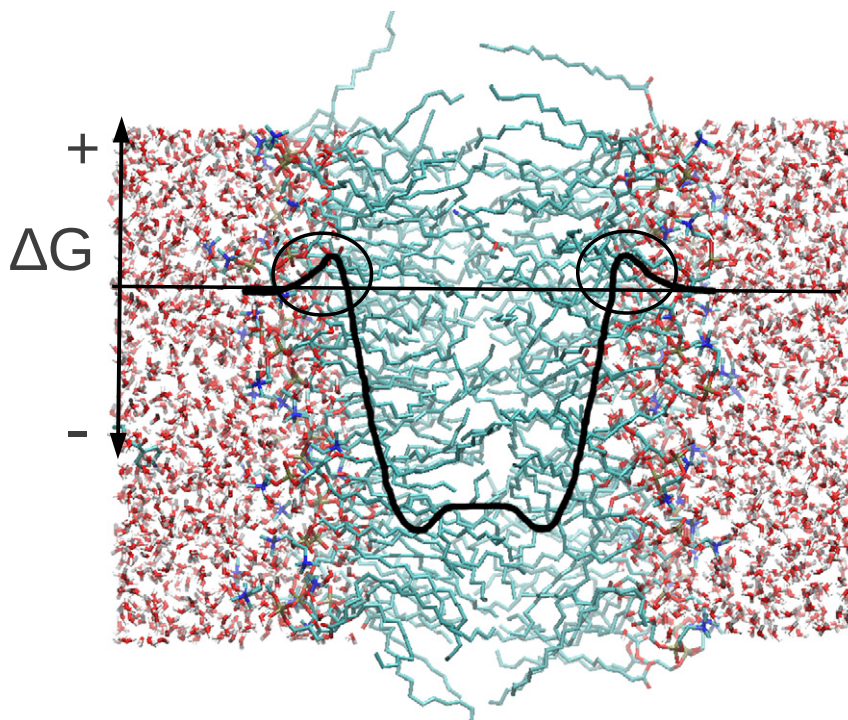


Fig. 2. Schematic representation of the free energy profile, $\Delta G(z)$ (solid line) associated with the insertion of a benzocaine molecule into the lipid bilayer of $\chi=0$, in the absence of salt. In this figure, both maxima of $\Delta G_{\max}(z)$ associated with the insertion process into the lipid bilayer located at the lipid/water interface are marked with circles.

this behaviour based on the variation in the interfacial tension of the phospholipid bilayer/solution with the phospholipid composition.

3.2. Lipid/water interfacial tension, γ^b

The interfacial tension measured experimentally can be related with the interfacial tension calculated by simulation using the equation [39],

$$\gamma^b = \gamma^r + \gamma^s \quad (7)$$

where γ^r represents the reference interfacial tension (in our case, the interfacial tension measured experimentally for the system dodecane +

water [40] due to its similarity to the lipid hydrocarbon tails involved in this study), and γ^s represents the interfacial tension calculated from simulation by integration of the lateral pressure profile across the lipid bilayer [41,30], as follows,

$$\gamma^s = -\frac{1}{2} \int_{-\infty}^{\infty} \pi(z) dz \quad (8)$$

where the zero of the Z-axis (normal to the lipid bilayer) is placed in the middle of the lipid bilayer, and $\pi(z)$ corresponds to the lateral pressure profile across the lipid bilayer.

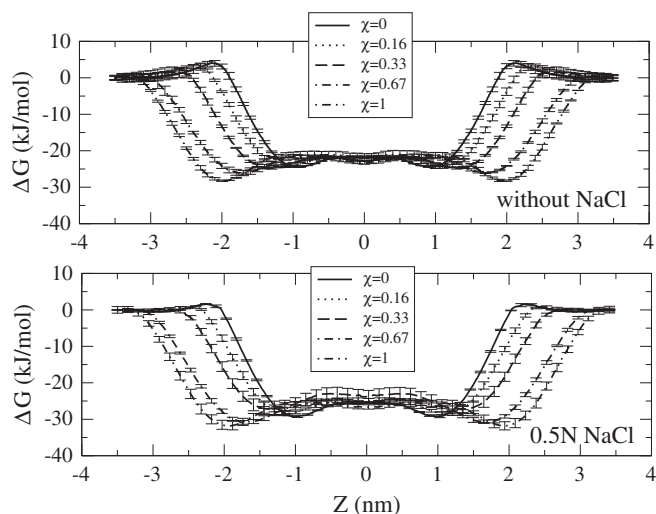


Fig. 3. Free energy profile, ΔG , associated with the insertion of a benzocaine molecule into the lipid bilayer as a function of the lipid membrane composition, χ . Zero is placed in the middle of the lipid bilayer. The error bars were calculated from 4 sub-trajectories of 10 ns length, after discarding the first 10 ns of simulation as equilibration time.

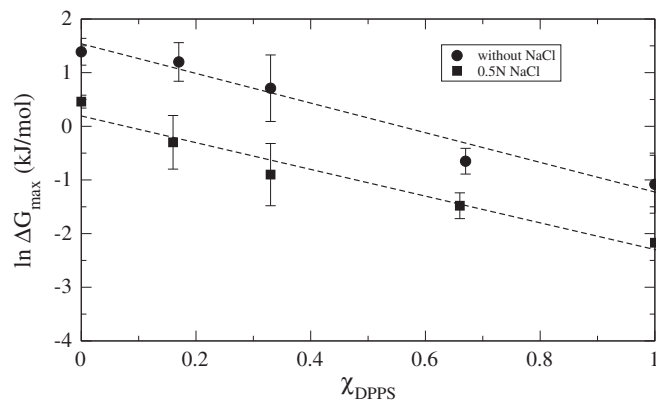


Fig. 4. Semi-logarithmic representation of the ΔG_{\max} (in Fig. 3) with respect to the membrane composition, χ . The error bars were calculated from 4 sub-trajectories of 10 ns length after discarding the first 10 ns of the simulation as equilibration time.

To compute the local pressure from the simulated trajectory, the instantaneous pressure must be calculated across the phospholipid bilayer every time step. Thus, the pressure tensor \mathbf{P} is expressed as

$$\mathbf{P} = \left(\sum_i m_i \mathbf{v}_i \otimes \mathbf{v}_i - \frac{1}{V} \sum_{i,j} F_{ij} \otimes \mathbf{r}_{ij} \right) \quad (9)$$

where the first term corresponds to the kinetic energy of the system, E_k , and the second term is related with the molecular virial of the system, Ξ ; m_i and \mathbf{v}_i correspond to the mass and velocity of each particle of the system, and finally, \mathbf{r}_{ij} and F_{ij} correspond to the distance and force between two particles, i – j , respectively. The pairwise interactions include non-bonded forces (electrostatic and van der Waals interactions) and covalent interactions between bonded atoms. Because pressure tensor \mathbf{P} is calculated in equilibrium, the terms of this tensor outside the diagonal can be ignored.

Since the electrostatic contribution using a long range electrostatic interaction by the Particle Mesh Ewald method [18,19] cannot be decomposed in F_{ij} terms, its contribution must be calculated using a cut-off method. In this regard, to calculate the pressure profile along the Z-axis perpendicular to the lipid bilayer, the \mathbf{P} tensor must be calculated for thin slices parallel to the membrane surface across the lipid bilayer; in our case, a thickness of roughly 0.1 nm was chosen for all our simulations. However, in certain circumstances (or even in most cases), the particles i – j may lie in different slices. In these cases, the Lindahl and Edholm [42] approximations can be used, and Eq. (9) was accordingly modified as follows:

$$P = \sum_{i \in \text{slice}} m_i \mathbf{v}_i \otimes \mathbf{v}_i - \frac{1}{\Delta V} \sum_{i,j} F_{ij} \otimes \mathbf{r}_{ij} f(z, z_i, z_j) \quad (10)$$

where the first term of this summatory corresponds to the kinetic contribution from all the particles that fall in the i -slice, ΔV is the volume associated with each slice of Δz thickness, and the $f(z, z_i, z_j)$ corresponds to a discrete function defined as follows:

- 1 If both particles fall in the same slice, $i, f=1$.
- 2 If both particles are outside slice i and on opposite sides, $f = \frac{\Delta z}{|z_i - z_j|}$
- 3 If one particle is in slice i and the other outside, $f = \frac{\Delta z}{2|z_i - z_j|}$

In this regard, the lateral pressure $\pi(z)$ along the Z-axis can be expressed as follows:

$$\pi(z) = p_{\text{lat}}(z) - p_N \quad (11)$$

where $p_N = p_{zz}$ and $p_{\text{lat}} = (p_{xx} + p_{yy})/2$, with p_{xx} , p_{yy} and p_{zz} the diagonal of the local pressure tensor defined in the Eq. (10). Hence, due to the isotropic behaviour in bulk solution (where there is no preferable direction), $\pi(z) = 0$. However, $\pi(z)$ in the bilayer or in its vicinity can adopt positive or negative values in different positions across the phospholipid bilayer. In this respect, Fig. 5 shows the lateral pressure profiles, $\pi(z)$, for different molecular fractions, χ , in the presence and absence of salt.

Table 1 shows the interfacial tension γ^b calculated for the different lipid bilayer compositions, χ . In the case of a bilayer formed only by DPPC, $\chi=0$, interfacial tensions of $\gamma^b = 38.1 \pm 0.8$ mN/m and 36.50 ± 0.07 mN/m were estimated from the simulation, in the absence of salt and with 0.5 N NaCl in the aqueous solution, respectively, values that are of the same order of magnitude as the value measured for the oil–water interface tension, where values of ≈ 40 mN/m have been reported [40,43]. Unlikely there are not experimental data to compare with, however these values agree with the simulation data calculated by Gullingsrud and Schulten [30], who reported values in a range from 27.6 ± 10 mN/m to 39.6 ± 1.6 mN/m for different surface areas of DOPC.

Furthermore, Table 1 shows how the interfacial tension increases with the fraction of DPPS in the lipid bilayer. This enhancement of

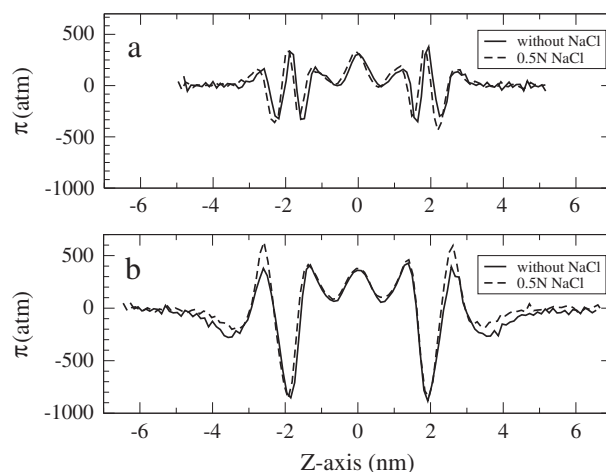


Fig. 5. Lateral pressure profile of a DPPC and DPPS bilayer, corresponding to $\chi=0$ and $\chi=1$, in the absence of salt (a) and with 0.5 N NaCl in solution (b), respectively.

the interfacial tension with the fraction of DPPS in the lipid bilayer is directly related with the increase in the dehydration of the lipid bilayer associated with increasing lipid–lipid molecular interactions, as was described in a previous work [39]. On the other hand, the presence of salt in the aqueous solution substantially changes the trend of the interface tension related with the fraction of DPPS in the lipid bilayer. Thus, in general, for the full range of fractions of DPPS in the lipid bilayer, the interfacial tension adopts always values below the interfacial tension of the reference, $\gamma^b < \gamma^r$ ($\gamma^r = 50$ mN/m [40]). Hence, the lipid–lipid interactions associated with the presence of DPPS in the lipid bilayer are partially screened by the ionic strength of the aqueous solution, so that γ^b reaches a plateau for a range of molecular fractions of DPPS between 0.2 and 1, with γ^b taking values of ≈ 43 mN/m in this range of DPPS molecular fractions.

This behaviour of the interfacial tension associated with the presence of salt in the aqueous solution and the molecular fraction of charged lipids in the lipid bilayer could well be of a great biological relevance, since at a given ionic strength of the aqueous solution, the interfacial tension of a cellular membrane becomes independent of the fraction of the charged lipids present in the membrane. This fact results of crucial importance considering the asymmetry in the molecular fraction of charged lipids between both leaflets of the membrane of a eukariotic cell, whereby the ionic strength could equal the interfacial tension between both sides of the membrane, even when they have different lipidic compositions.

3.3. Dependence of the free energy barrier on interfacial tension

Fig. 6 depicts a semi-logarithmic representation of the free energy associated with the insertion of the benzocaine into a lipid bilayer versus the interfacial tension of the lipid bilayer for several molecular fractions χ of the lipid bilayer.

Fig. 6 shows how the free energy barrier associated with the insertion of benzocaine into a lipid bilayer fits a straight line representing

Table 1

Interfacial tension for different molecular fractions χ of the lipid bilayer. Error bars were calculated from 3 sub-trajectories of 30 ns each, where the first 10 ns of the simulation trajectory were discarded as being the equilibration time.

χ	$\gamma_{\text{without NaCl}}^b$ (mN/m)	$\gamma_{0.5 \text{ N NaCl}}^b$ (mN/m)
0	38.0 ± 0.8	36.51 ± 0.12
0.16	49.90 ± 0.14	41.91 ± 0.09
0.33	55.1 ± 0.9	43.610 ± 0.003
0.66	69.0 ± 1.4	43.101 ± 0.002
1	73.2 ± 0.7	44.310 ± 0.006

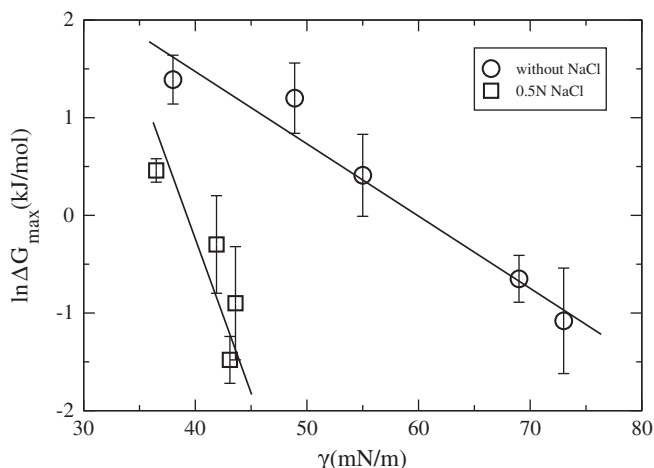


Fig. 6. ΔG_{\max} vs. the interfacial surface tension in the phospholipid bilayer corresponding to different fractions χ of the lipid composition in the phospholipid bilayer. Error bars were calculated from 3 sub-trajectories of 30 ns each, where the first 10 ns of the simulation trajectory were discarded as being the equilibration time.

the interfacial tension in a semi-logarithmic form. This behaviour is explained by assuming that the increasing dehydration of the interface as the fraction of DPPS increases (due to the greater exposure of the hydrophobic parts of the phospholipids to the solution), the energy required to pass through this zone by the benzocaine (a neutral molecule very insoluble in aqueous solution) is reduced.

Finally, the expression obtained for the free energy barrier as a function of the interfacial tension is as follows:

$$\ln \Delta G_{\max} = -0.074\gamma + 4.47 \text{ (without NaCl)} \quad (12)$$

$$\ln \Delta G_{\max} = -0.283\gamma + 10.95 \text{ (0.5 N NaCl)}. \quad (13)$$

Thus, we observe how the thermodynamic barrier associated with benzocaine insertion into a lipid bilayer depends exponentially on the interfacial tension between the phospholipid bilayer and the aqueous solution. The barrier diminishing as the ionic strength of the aqueous solution increases.

3.4. Concluding remarks

Understanding the molecular mechanism that controls the insertion of a local anaesthetic into a lipid bilayer is of undoubted importance for describing the activity of these drugs. In this respect, it is clinically known, how the potency and activity of local anaesthetics increase when these drugs are dissolved in a sodium bicarbonate buffer. One of the main factors related with this increase in potency has been associated with the reduction on the protonated form on the local anaesthetic in the equilibrium. However, to the best of our knowledge, almost no attention has been paid about the role played by the increase in the ionic strength of the buffer solution in which the anaesthetic was dissolved.

In this context, this work was focused on studying the thermodynamic barrier associated with the insertion of benzocaine into binary lipid bilayers of DPPC/DPPS, it being found that this barrier exponentially diminished with the increasing molecular fraction of charged lipids that form the membrane. In addition, it was also observed how an increase in the ionic strength of the lipid bilayer produced an additional reduction in this thermodynamic barrier. The increase in the interfacial tension between the phospholipid bilayer and the aqueous solution would explain this molecular behaviour, which is strongly dependent on the phospholipid fraction χ that forms the lipid bilayer, and the absence or the presence of salt in the aqueous solution.

However, further studies should be carried out to approach our simulations to the real structure of a cell membrane, such as the consideration of the presence of cholesterol in the model, due to the role played by cholesterol on the structure of the lipid bilayer, i.e., on the insertion of local anaesthetics into a cell membrane.

Acknowledgements

The authors wish to thank Centro de Calculo Cientifico of the Universidad Politecnica de Cartagena for their support in carrying out the calculations on which this work is based.

References

- [1] T. Narahashi, D. Frazier, M. Yamada, The site of action and active form of local anesthetics. I. Theory and pH experiments with tertiary compounds, *Journal of Pharmacology and Experimental Therapeutics* 171 (1972) 32–44.
- [2] R. de Jong, Book: Local Anesthetics, Mosby, 1994.
- [3] L. Pinto, D. Yokaihiya, L. Fracedo, E. de Paula, Interaction of benzocaine with model membranes, *Biophysical Chemistry* 87 (2000) 213–223.
- [4] H. Matsuki, T. Hata, M. Yamanaka, S. Kaneshina, Partitioning of uncharged local anesthetic benzocaine into model biomembranes, *Colloids and Surfaces B* 22 (1) (2001) 69–76.
- [5] W. McKay, R. Morris, M. Faracs, P. Mushlin, Sodium bicarbonate attenuates pain on skin infiltration with lidocaine, with or without epinephrine, *Anesthesia and Analgesia* 66 (6) (1987) 572–574.
- [6] K. Zahl, A. Jordan, J. McGroarty, B. Sorensen, A. Gotta, Peribulbar anesthesia – effect of bicarbonate on mixtures of lidocaine, bupivacaine, and hyaluronidase with or without epinephrine, *Ophthalmology* 98 (2) (1991) 239–242.
- [7] J. Ritchie, B. Ritchie, Local anesthetics: effect of pH on activity, *Science* 162 (1968) 1394–1395.
- [8] A. Shibata, K. Maeda, H. Ikema, S. Ueno, Y. Suezaki, S. Liu, Y. Baba, I. Ueda, Local anesthetics facilitate ion transport across lipid planar bilayer membranes under an electric field: dependence on type of lipid bilayer, *Colloids and Surfaces B* 42 (2005) 197–203.
- [9] R.D. Porasso, W.F.D. Bennett, S.D. Oliveira-Costa, J. López Cascales, Study of the benzocaine transfer from aqueous solution to the interior of a biological membrane, *The Journal of Physical Chemistry. B* 113 (29) (2009) 9988–9994.
- [10] J.L. Cascales, S. Oliveira-Costa, R. Porasso, Thermodynamic study of benzocaine insertion into different lipid bilayers, *Journal of Chemical Physics* 135 (13) (2011) 135,103–135,107.
- [11] H.J.C. Berendsen, J.P.M. Postma, W.F. van Gunsteren, J. Hermans, *Intermolecular Forces*, D. Reidel Publishing Company, 1981.
- [12] J.J. López Cascales, J. García de la Torre, S. Marrink, H. Berendsen, Molecular dynamics simulation of a charged biological membrane, *Journal of Chemical Physics* 104 (7) (1996) 2713–2720.
- [13] J. López Cascales, H. Berendsen, J. Garcia de la Torre, *Journal of Physical Chemistry* 100 (21) (1996) 8621–8627.
- [14] J. López Cascales, M. Huertas, J. de la Torre, Molecular dynamics simulation of a dye molecule in the interior of a bilayer: 1,6-diphenyl-1,3,5-hexatriene in dipalmitoylphosphatidylcholine, *Biophysical Journal* 69 (1) (1997) 1–8.
- [15] J.A. Pople, G.A. Segal, Approximate self-consistent molecular orbital theory. 3. CNDO results for AB2 and AB3 systems, *Journal of Chemical Physics* 44 (9) (1966) 3289.
- [16] H.J.C. Berendsen, D. Van Der Spoel, R. Van Drunen, Gromacs – a message-passing parallel molecular-dynamics implementation, *Computer Physics Communications* 91 (1–3) (1995) 43–56.
- [17] E. Lindahl, B. Hess, D. van der Spoel, Gromacs 3.0: a package for molecular simulation and trajectory analysis, *Journal of Molecular Modeling* 7 (8) (2001) 306–317.
- [18] T. Darden, D. York, L. Pedersen, Particle mesh Ewald – an N.log(N) method for Ewald sums in large systems, *Journal of Chemical Physics* 98 (12) (1993) 10,089–10,092.
- [19] U. Essmann, L. Perera, M.B.T. Darden, H. Lee, L. Pedersen, A smooth particle mesh Ewald method, *Journal of Chemical Physics* 103 (19) (1995) 8577–8593.
- [20] B. Hess, H. Bekker, H. Berendsen, H.J.C. Fraaije, LINC: a linear constraint solver for molecular simulations, *Journal of Computational Chemistry* 18 (1997) 1463–1472.
- [21] H.J.C. Berendsen, J.P.M. Postma, W.F. van Gunsteren, A. DiNola, J.R. Haak, Molecular dynamics with coupling to an external bath, *Journal of Chemical Physics* 81 (8) (1984) 3684–3690.
- [22] A. Seeling, J. Seeling, The dynamic structure of fatty acyl chains in a phospholipid bilayer measured by deuterium magnetic resonance, *Biochemistry* 23 (1974) 4839–4845.
- [23] G. Cevc, A. Watts, D. Marsh, Titration of the phase transition of phosphatidylserine bilayer membranes. Effect of pH, surface electrostatics, ion binding and head-group hydration, *Biochemistry* 20 (1981) 4955–4965.
- [24] E. Luna, H. McConnell, Lateral phase separations in binary-mixtures of phospholipids having different charges and different crystalline-structures, *Biochimica et Biophysica Acta* 470 (1977) 303–316.
- [25] E. Egberts, S.J. Marrink, H.J.C. Berendsen, Molecular dynamics simulation of a phospholipid membrane, *European Biophysics Journal* 22 (6) (1994) 423–436.

- [26] J. Lopez Cascales, J. Garcia de la Torre, Effect of lithium and sodium ions on a charged membrane of dipalmitoylphosphatidylserine: a study by molecular dynamics simulations, *Biochimica et Biophysica Acta* 1330 (2) (1997) 145–156.
- [27] R. Porasso, J. López Cascales, Study of the effect of Na^+ and Ca^{2+} ion concentration on the structure of an asymmetric DPPC/DPPC + DPPS lipid bilayer by molecular dynamics simulation, *Colloids and Surfaces. B, Biointerfaces* (73) (2009) 42–50.
- [28] B. Jonsson, O. Edholm, O. Teleman, Molecular dynamics simulation of a sodium octanoate micelle in aqueous-solution, *Journal of Chemical Physics* (85) (1986) 2259–2271.
- [29] W.F. van Gunsteren, H.J.C. Berendsen, GROMOS: GRoningen MOlecular Simulation is a software package, *Biomos, Nijenborgh* 4, 9747AG Groningen, The Netherlands, 1987.
- [30] J. Gullingsrud, K. Schulten, Lipid bilayer pressure profiles and mechanosensitive channel gating, *Biophysical Journal* 86 (2004) 3496–3509.
- [31] J. Sonne, F. Hansen, G. Peters, Methodological problems in pressure profile calculations for lipid bilayers, *Journal of Chemical Physics* 122 (12) (2005) 1–9, (124903).
- [32] M. Patra, Lateral pressure profiles in cholesterol-DPPC bilayers, *European Biophysics Journal* 35 (1) (2005) 79–88.
- [33] G. Torrie, J. Valleau, Nonphysical sampling distribution in Monte Carlo free-energy estimation umbrella sampling, *Journal of Computational Physics* 23 (2) (1977) 187–199.
- [34] S. Kumar, D. Bouzida, R. Swensen, P. Kollman, J. Rosemberg, The weighted histogram analysis method for free-energy calculations on biomolecules. I. The method, *Journal of Computational Chemistry* 13 (8) (1992) 1011–1021.
- [35] J. Maccallum, W.D. Bennett, D. Tieleman, Partitioning of acid side chains into lipid bilayers: results from computer simulations and comparison to experiment, *Journal of General Physiology* 129 (5) (2007) 371–377.
- [36] J.G. Casares, L. Camacho, M.M. Romero, J. López Cascales, Methylene blue adsorption on a DMPA lipid Langmuir monolayer, *ChemPhysChem* 11 (10) (2010) 2241–2247.
- [37] J. Lopez Cascales, S. Oliveira Costa, B. de Groot, E. Walters, Mechanical properties of binary DPPC/DPPS bilayers, *Biophysical Chemistry* 152 (1–3) (2010) 139–144.
- [38] J. Baenziger, M.-L. Morris, T. Darsaut, S. Ryan, Effect of membrane lipid composition on the conformational equilibria of the nicotinic acetylcholine receptor, *Journal of Biological Chemistry* 275 (2) (2000) 777–784.
- [39] J.J. López Cascales, S.D. Oliveira Costa, A. Garro, R.D. Enriz, Mechanical properties of binary DPPC/DPPS bilayers, *Royal Society of Chemistry Advances* 2 (2012) 11,743–11,750.
- [40] S. Zeppieri, J. Rodriguez, A. Lopez-de-Ramos, Interfacial tension of alkane + water systems, *Journal of Chemical & Engineering Data* 46 (2001) 1086–1088.
- [41] J. Rowlinson, B. Widom, *Molecular Theory of Capillarity*, Oxford University Press, 1982.
- [42] E. Lindahl, O. Edholm, Spatial and energetic–entropic decomposition of surface tension in lipid bilayers from molecular dynamics simulations, *Journal of Chemical Physics* 113 (9) (2000) 3882–3893.
- [43] E. Evans, W. Rawicz, Elasticity of fuzzy biomembranes, *Physical Review Letters* 79 (12) (1997) 2379–2382.